

Blazar Heating – The Rosetta Stone for Structure Formation?

Christoph Pfrommer¹

in collaboration with

Avery E. Broderick², Phil Chang², Ewald Puchwein¹, Volker Springel¹

¹Heidelberg Institute for Theoretical Studies, Germany

²Canadian Institute for Theoretical Astrophysics, Canada

Jul 26, 2011 / Lorentz Center Workshop



Outline

- 1 Physics of blazar heating
 - TeV emission from blazars
 - Propagation of TeV photons
 - Plasma instabilities
- 2 The intergalactic medium
 - Properties of blazar heating
 - Thermal history of the IGM
 - The Lyman- α forest
- 3 Structure formation
 - Entropy evolution
 - Bimodality of galaxy clusters
 - Formation of dwarf galaxies



Outline

- 1 Physics of blazar heating
 - TeV emission from blazars
 - Propagation of TeV photons
 - Plasma instabilities
- 2 The intergalactic medium
 - Properties of blazar heating
 - Thermal history of the IGM
 - The Lyman- α forest
- 3 Structure formation
 - Entropy evolution
 - Bimodality of galaxy clusters
 - Formation of dwarf galaxies



TeV gamma-ray astronomy

H.E.S.S.



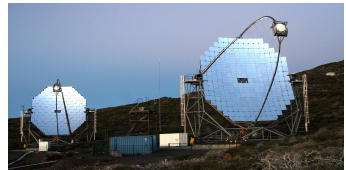
MAGIC I



VERITAS



MAGIC II

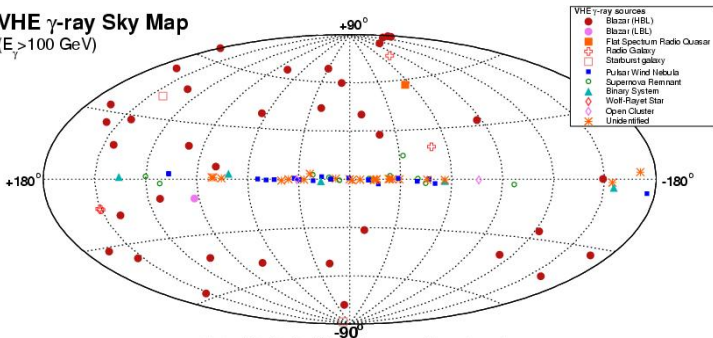


The TeV gamma-ray sky

There are several classes of TeV sources:

- Galactic - pulsars, BH binaries, supernova remnants
- Extragalactic - **mostly** blazars, two starburst galaxies

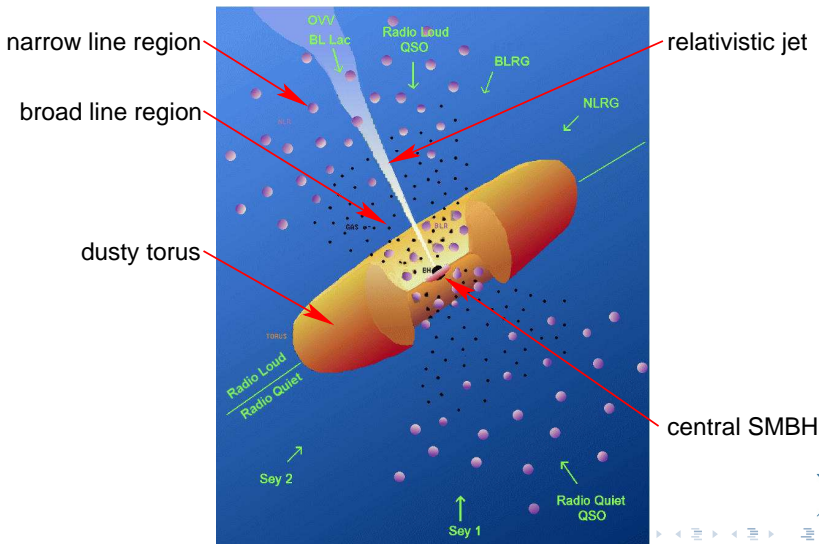
VHE γ -ray Sky Map
($E_{\gamma} > 100$ GeV)



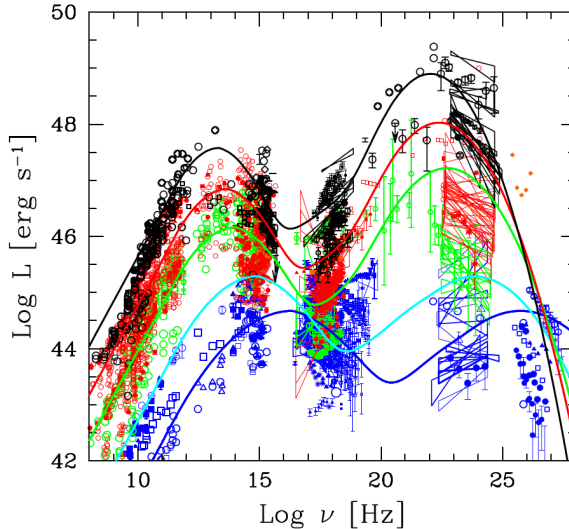
2011-01-08 - Up-to-date plot available at <http://www.inpp.mpg.de/~rwagne/s/sources/>



Unified model of active galactic nuclei



The blazar sequence



Ghisellini (2011)

Propagation of TeV photons

- 1 TeV photons can pair produce with 1 eV photons:

$$\gamma + \gamma \rightarrow e^+ + e^-$$

- mean free path for this depends on the density of 1 eV photons:
 - typically ~ 100 Mpc
 - pairs produced with energy of 0.5 TeV ($\gamma = 10^6$)
- these pairs inverse Compton scatter off the CMB photons
 - mean free path is ~ 30 kpc
 - producing gamma-rays of ~ 1 GeV

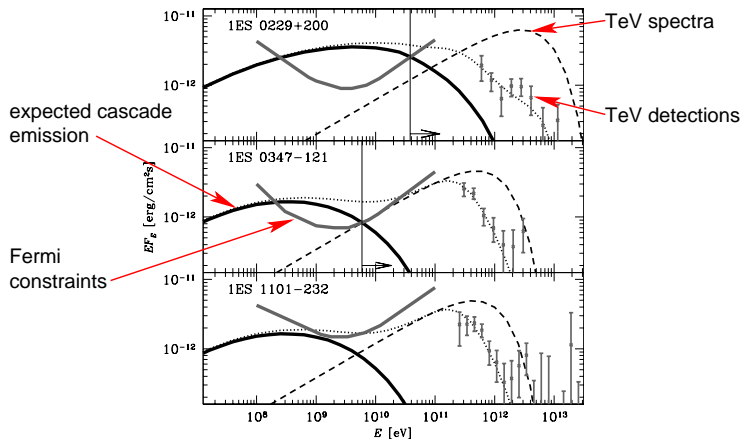
$$E \sim \gamma^2 E_{\text{CMB}} \sim 1 \text{ GeV}$$

- each TeV point source is also a GeV point source



What about the cascade emission?

Every TeV source should be associated with a 1-100 GeV gamma-ray halo – **not seen!**



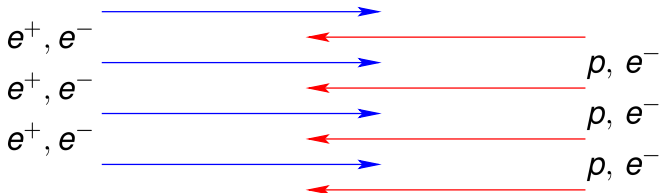
Neronov & Vovk (2010)



Missing plasma physics?

How do beams of e^+/e^- propagate through the IGM?

- plasma processes are important
- interpenetrating beams of charged particles are unstable
- consider the two-stream instability for two beams:



- one frequency (timescale) and one length in the problem:

$$\frac{\omega_p}{\gamma} = \sqrt{\frac{4\pi e^2 n_e}{\gamma^2 m_e}}$$

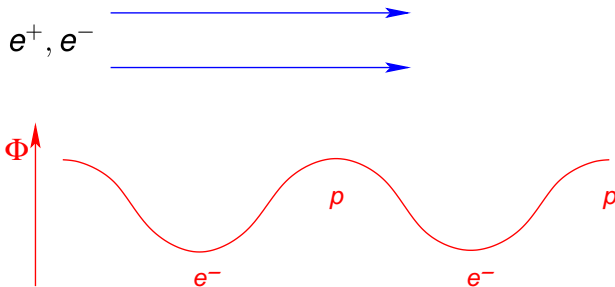
$$\lambda_p = \frac{\gamma c}{\omega_p}$$



Two-stream instability: mechanism

wave-like perturbation with $\mathbf{k} \parallel \mathbf{v}_{\text{beam}}$, longitudinal charge oscillations in background plasma (Langmuir wave):

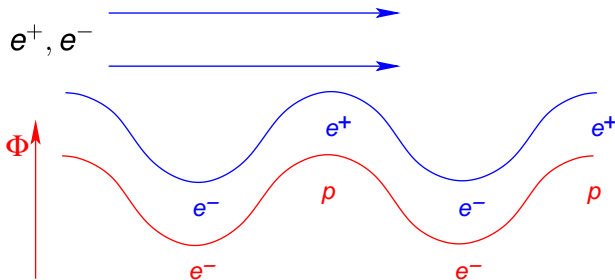
- initially homogeneous beam- e^- :
attractive (repulsive) force by potential maxima (minima)
- e^- attain lowest velocity in potential minima \rightarrow bunching up
- e^+ attain lowest velocity in potential maxima \rightarrow bunching up



Two-stream instability: mechanism

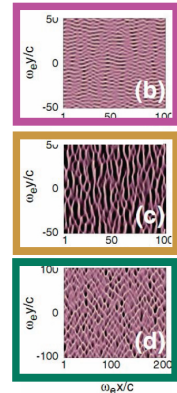
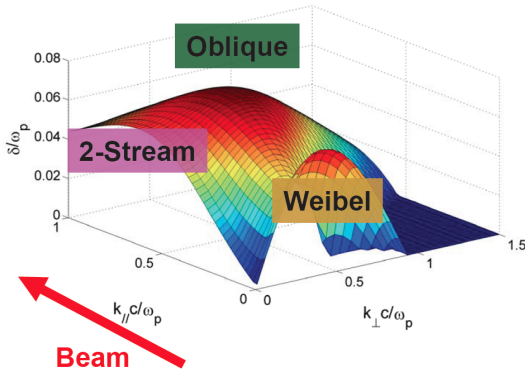
wave-like perturbation with $\mathbf{k} \parallel \mathbf{v}_{\text{beam}}$, longitudinal charge oscillations in background plasma (Langmuir wave):

- beam- e^+ / e^- couple in phase with the background perturbation: enhances background potential
- stronger forces on beam- $e^+ / e^- \rightarrow$ positive feedback
- exponential wave-growth \rightarrow instability



Oblique instability

k oblique to \mathbf{v}_{beam} : real world perturbations don't choose "easy" alignment = \sum all orientations

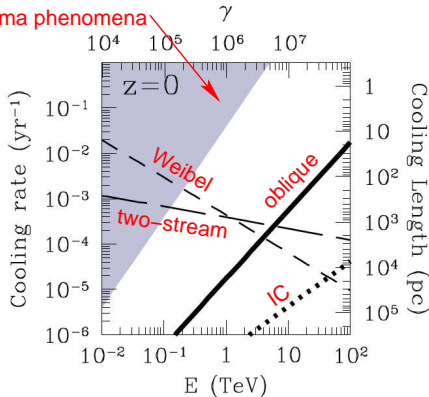


Bret (2009), Bret+ (2010)



Beam physics – growth rates

excluded for collective
 plasma phenomena



- consider a light beam penetrating into relatively dense plasma

- maximum growth rate

$$\sim 0.4 \gamma \frac{n_{\text{beam}}}{n_{\text{IGM}}} \omega_p$$

- oblique instability beats IC by two orders of magnitude

Broderick, Chang, C.P. (2011)



Beam physics – growth rates

- non-linear evolution of these instabilities at these density contrasts is not known
- expectation from PIC simulations suggest substantial isotropization of the beam
- plasma instabilities cool the beam, no energy left over for IC off the CMB

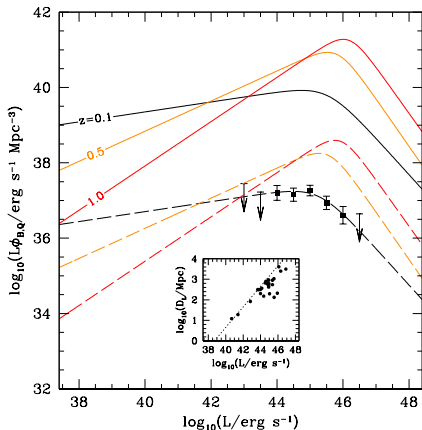


Outline

- 1 Physics of blazar heating
 - TeV emission from blazars
 - Propagation of TeV photons
 - Plasma instabilities
- 2 The intergalactic medium
 - Properties of blazar heating
 - Thermal history of the IGM
 - The Lyman- α forest
- 3 Structure formation
 - Entropy evolution
 - Bimodality of galaxy clusters
 - Formation of dwarf galaxies



TeV blazar luminosity density

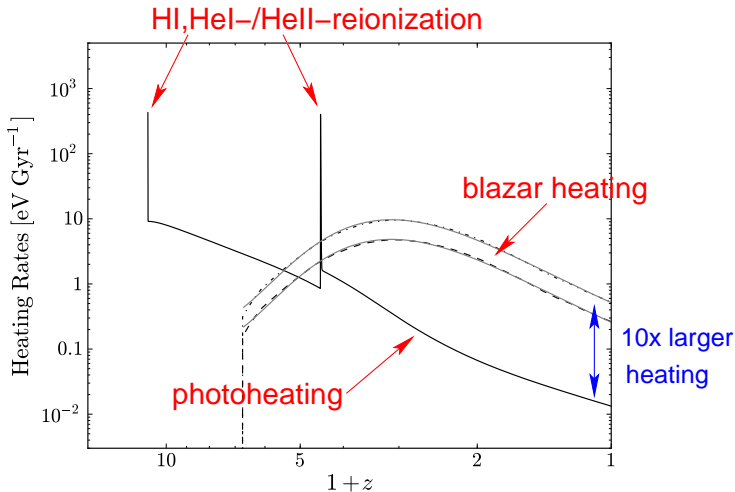


Broderick, Chang, C.P. (2011)

- collect luminosity of all 23 TeV blazars with good spectral measurements
- account for the selection effects
- TeV blazar luminosity density is a scaled version ($\sim 0.2\%$) of that of quasars!
- assume that they trace each other for all z



Evolution of the heating rates



Chang, Broderick, C.P. (2011)



Blazar heating vs. photoheating

- total power from AGN/stars vastly exceeds the TeV power of blazars
- $T_{\text{IGM}} \sim 10^4$ K (1 eV) at mean density ($z \sim 2$)

$$\varepsilon_{\text{th}} = \frac{kT}{m_p c^2} \sim 10^{-9}$$

- radiative energy ratio emitted by BHs in the Universe (Fukugita & Peebles 2004)

$$\varepsilon_{\text{rad}} = \eta \Omega_{\text{bh}} \sim 0.1 \times 10^{-4} \sim 10^{-5}$$

- fraction of the energy energetic enough to ionize H I is ~ 0.1 :

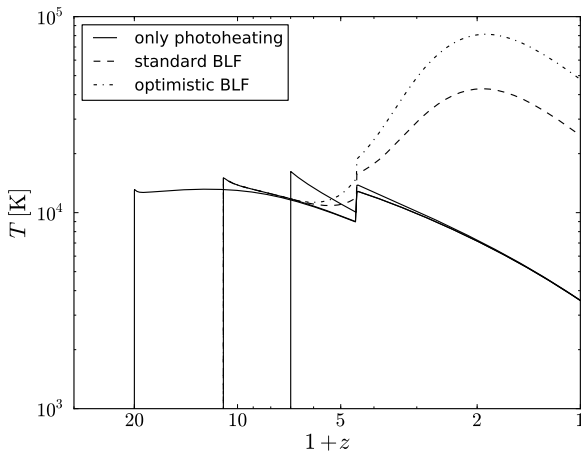
$$\varepsilon_{\text{UV}} \sim 0.1 \varepsilon_{\text{rad}} \sim 10^{-6} \quad \rightarrow \quad kT \sim \text{keV}$$

- photoheating efficiency $\eta_{\text{ph}} \sim 10^{-3} \quad \rightarrow \quad kT \sim \eta_{\text{ph}} \varepsilon_{\text{UV}} m_p c^2 \sim \text{eV}$
 (limited by the abundance of H I/He II due to the small recombination rate)

- blazar heating efficiency $\eta_{\text{bh}} \sim 10^{-3} \quad \rightarrow \quad kT \sim \eta_{\text{bh}} \varepsilon_{\text{rad}} m_p c^2 \sim 10 \text{ eV}$
 (limited by the total power of TeV sources)



Thermal history of the IGM

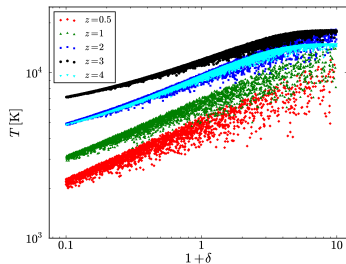


Chang, Broderick, C.P. (2011)

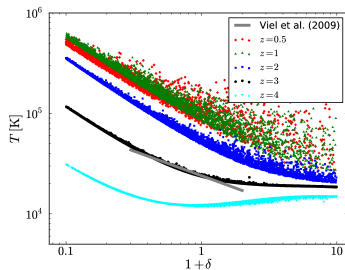


Evolution of the equation of state

no blazar heating



blazar heating



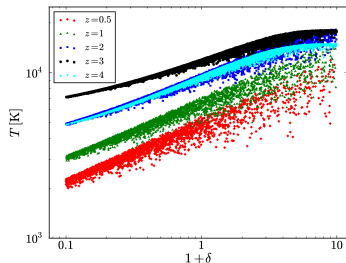
Chang, Broderick, C.P. (2011)

- blazars and extragalactic background light are uniform
→ blazar heating independent of density
→ causes inverted equation of state, $T \propto 1/\delta$
- blazars completely change the thermal history of the diffuse IGM and late-time structure formation

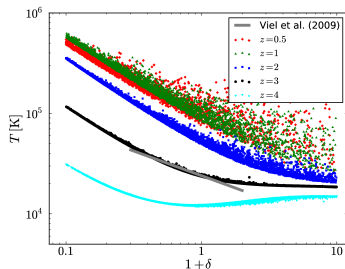


Evolution of the equation of state

no blazar heating



blazar heating

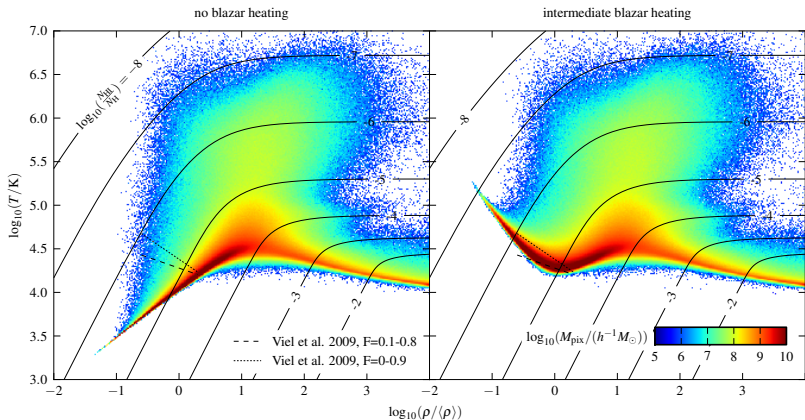


Chang, Broderick, C.P. (2011)

- blazars and extragalactic background light are uniform
→ blazar heating independent of density
→ causes inverted equation of state, $T \propto 1/\delta$
- blazars completely change the thermal history of the diffuse IGM and late-time structure formation



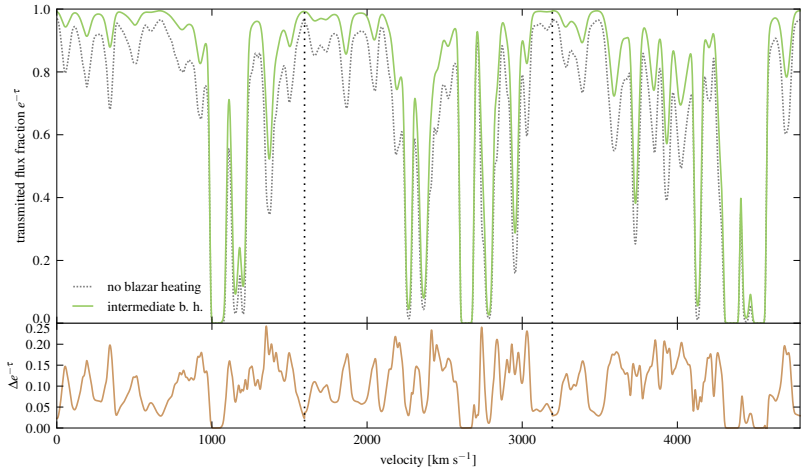
Equation of state



Puchwein, C.P., Springel, Broderick, Chang (2011)



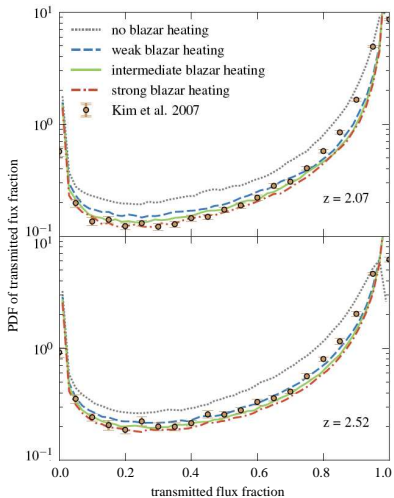
Ly- α spectra



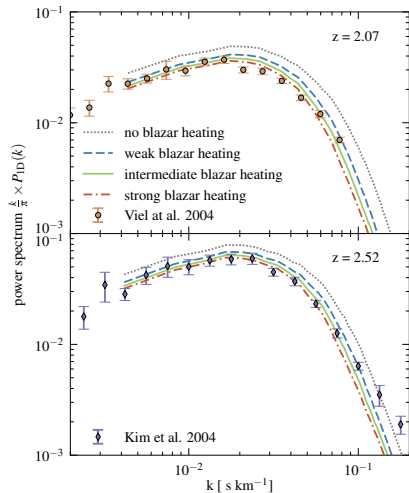
Puchwein+ (2011)



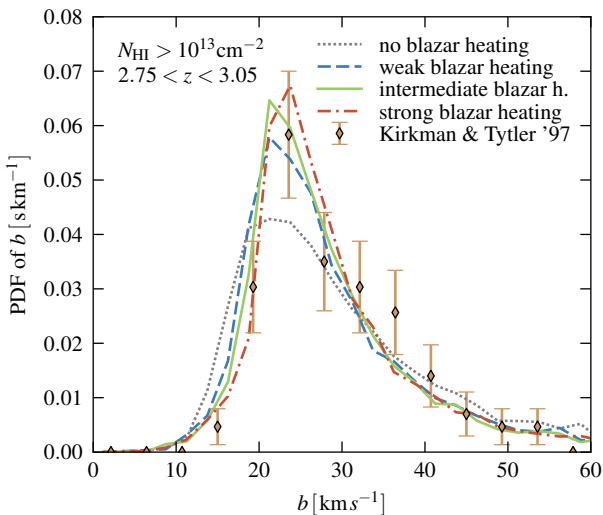
Ly- α flux PDFs and power spectra



Puchwein+ (2011)



Voigt profile fitting – line width distribution



Puchwein+ (2011)



Lyman- α forest in a blazar heated Universe

impressive improvement in modelling the Lyman- α forest is a direct consequence of the peculiar properties of blazar heating:

- **heating rate independent of IGM density** \rightarrow naturally produces the inverted EOS that Lyman- α forest data demand
- **recent and continuous nature of the heating** needed to match the redshift evolutions of all Lyman- α forest statistics
- **magnitude of the heating rate required by Lyman- α forest data**
 \sim **the total energy output of TeV blazars** (or equivalently $\sim 0.2\%$ of that of quasars)



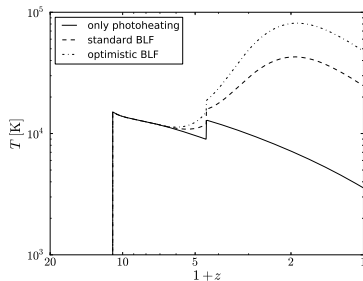
Outline

- 1 Physics of blazar heating
 - TeV emission from blazars
 - Propagation of TeV photons
 - Plasma instabilities
- 2 The intergalactic medium
 - Properties of blazar heating
 - Thermal history of the IGM
 - The Lyman- α forest
- 3 **Structure formation**
 - Entropy evolution
 - Bimodality of galaxy clusters
 - Formation of dwarf galaxies

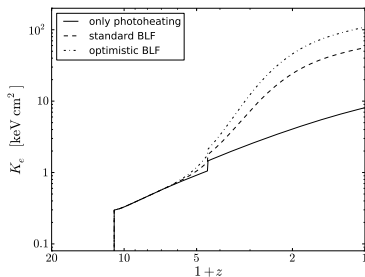


Entropy evolution

temperature evolution



entropy evolution



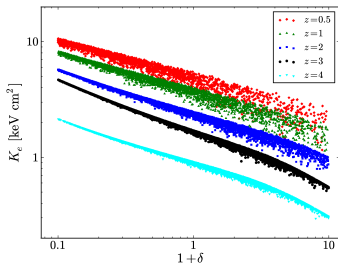
C.P., Chang, Broderick (2011)

- evolution of the entropy, $K_e = kTn_e^{-2/3}$, at mean density
- blazar heating substantially increases the entropy floor ($z \lesssim 2$)

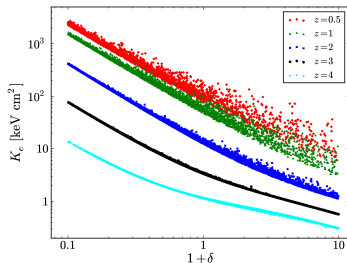


Evolution of the entropy equation of state

no blazar heating



blazar heating



C.P., Chang, Broderick (2011)

- blazar heating substantially increases the entropy in voids
- scatter is also increased \rightarrow larger stochasticity of structure formation



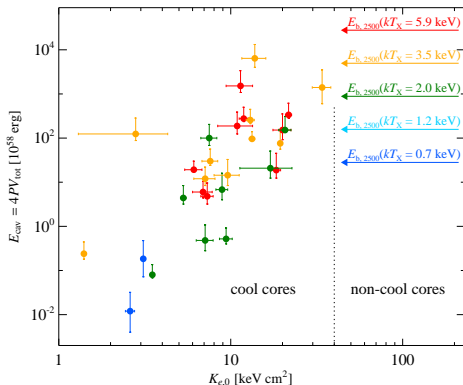
Blazar heating: AGN feedback vs. pre-heating

Blazar heating is an amalgam of pre-heating and AGN feedback:

- **blazar heating is not localized** (\neq AGN feedback)
→ changes initial conditions for forming groups (but provides no stability for cool cores, CCs)
- **blazar heating generates time-dependent entropy floor** (\neq pre-heating)
→ solves the classical problems of pre-heating ($z \sim 3$):
 - provides a physical mechanism
 - does not starve galaxy formation for $z \lesssim 3$
 - early forming groups can cool and develop observed low- K_e cores



How efficient is heating by AGN feedback?



C.P., Chang, Broderick (2011)

- on a buoyancy timescale, no AGN outburst transforms a CC to a non-cool core (NCC) cluster!

- cavity enthalpy

$$E_{\text{cav}} = 4 PV_{\text{tot}}$$

- in some cases

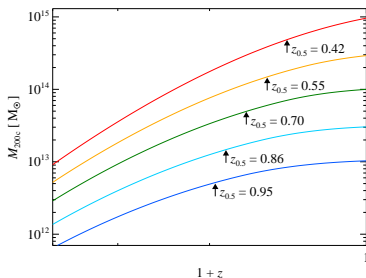
$$E_{\text{cav}} \gtrsim E_{\text{bind}}(R_{2500})$$

- cavity energy only couples weakly into ICM, but prevents cooling catastrophe

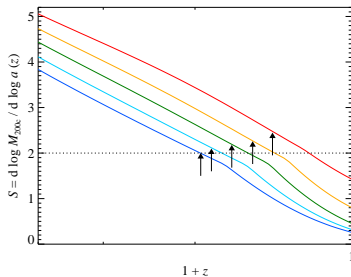


Mass accretion history of groups/clusters

mass accretion history



mass accretion rates



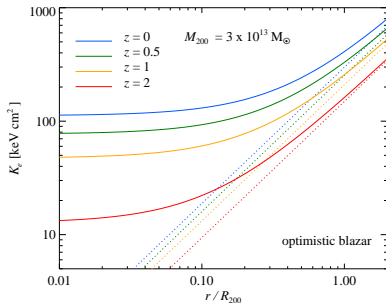
C.P., Chang, Broderick (2011)

- peak entropy injection from blazar heating ($z \sim 1$) matches formation time of groups
- early forming groups are unaffected and develop cool cores
- late forming groups have an elevated entropy core

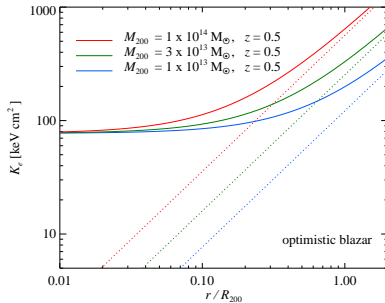


Entropy profiles: effect of blazar heating

varying formation time



varying cluster mass



C.P., Chang, Broderick (2011)

- cluster entropy profile immediately after formation (no cooling)
- largest effect for late forming, small objects

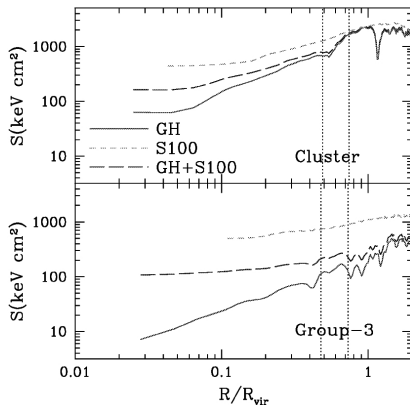


Scenario for the bimodality of cluster core entropies ?

- entropy core, $K_{e,0}$, immediately after formation is set by the z -dependent blazar heating
- only late forming groups ($z \lesssim 1$) are directly affected by blazar (pre-)heating
- if the cooling time, t_{cool} , is shorter than the time period to the successive merger, t_{merger} , the group will radiate away the elevated core entropy and evolve into a CC
- if $t_{\text{cool}} > t_{\text{merger}}$, merger shocks can gravitationally reprocess the entropy cores and amplify them \rightarrow potentially those forming clusters evolve into non-cool core (NCC) systems



Gravitational reprocessing of entropy floors

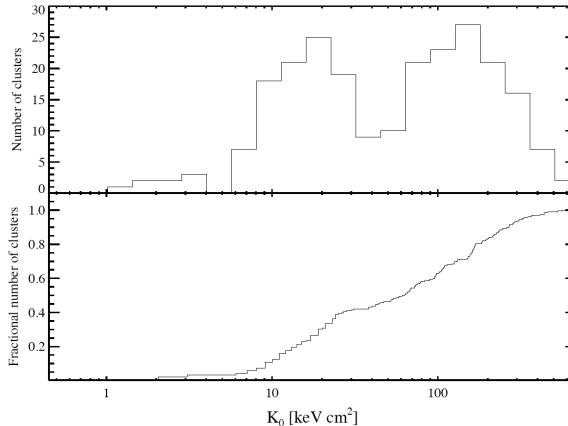


Borgani+ (2005)

- larger $K_{e,0}$ of a merging cluster facilitates shock heating \rightarrow increase of $K_{e,0}$ over entropy floor
- entropy floor of 100 keV cm^2 at $z = 3$ in non-radiative simulation:
net entropy amplification factor $\sim 3\text{--}5$ for clusters and groups (Borgani+ 2005)
- expect median of $K_{e,0} \sim 150 \text{ keV cm}^2$; maximum $K_{e,0} \sim 600 \text{ keV cm}^2$



Bimodality of cluster core entropies



Cavagnolo+ (2009)

- *Chandra* observations match blazar heating expectations!
- need hydrodynamic simulations to confirm this scenario



Jeans mass

- on small enough scales, the thermal pressure can oppose gravitational collapse of the gas
- characteristic length scale below which objects will not form
- Jeans wavenumber and mass is obtained by balancing the sound crossing and free-fall timescales

$$k_J(a) \equiv \frac{a}{c_s(a)} \sqrt{4\pi G \bar{\rho}(a)}$$

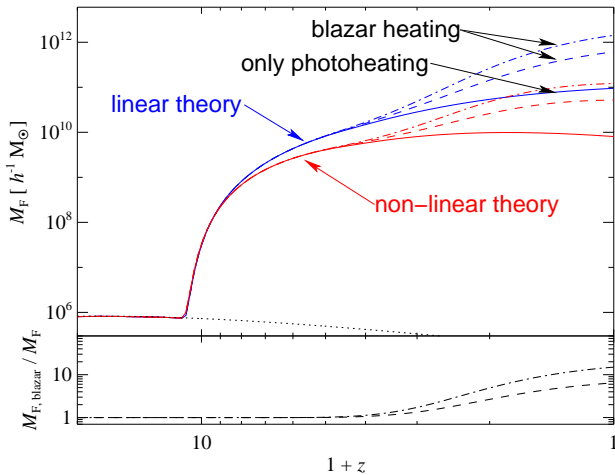
$$M_J(a) \equiv \frac{4\pi}{3} \bar{\rho}(a) \left(\frac{2\pi a}{k_J(a)} \right)^3 = \frac{4\pi^{5/2}}{3} \frac{c_s^3(a)}{G^{3/2} \bar{\rho}^{1/2}(a)}$$

- blazar heating increases the IGM temperature by ~ 10 :

$$\frac{M_{J,\text{blazar}}}{M_{J,\text{photo}}} = \left(\frac{c_{s,\text{blazar}}}{c_{s,\text{photo}}} \right)^3 = \left(\frac{T_{\text{blazar}}}{T_{\text{photo}}} \right)^{3/2} \gtrsim 30$$



Filtering mass – dwarf formation

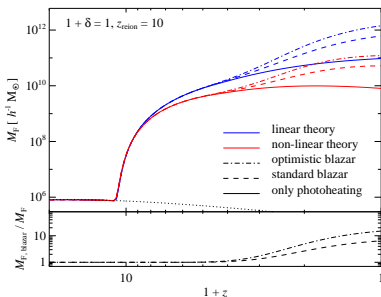


C.P., Chang, Broderick (2011)

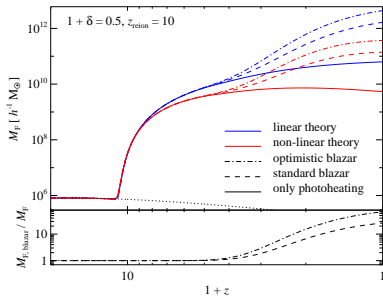


Peebles' void phenomenon explained?

mean density



void, $1 + \delta = 0.5$



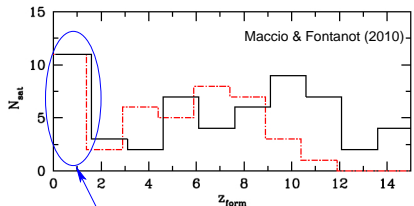
C.P., Chang, Broderick (2011)

- blazar heating efficiently suppresses the formation of void dwarfs within existing DM halos of masses $< 3 \times 10^{11} M_\odot$ ($z = 0$)
- reconciling the number of void dwarfs in simulations and the paucity of those in observations



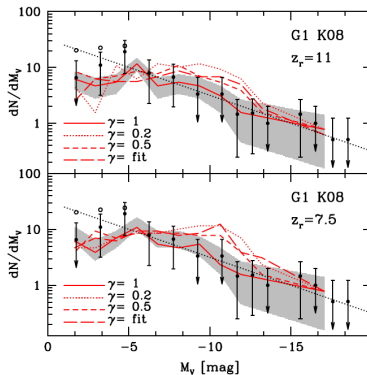
“Missing satellite” problem in the Milky Way

satellite formation time



late forming satellites (< 10 Gyr)
 not observed!

satellite luminosity function



Maccio+ (2010)

- blazar heating suppresses late satellite formation, reconciling low observed dwarf abundances with CDM simulations



Conclusions on blazar heating

- **novel mechanism; dramatically alters thermal history of the IGM:**
 - uniform and z -dependent preheating
 - rate independent of density \rightarrow inverted EOS
 - consistent picture of Lyman- α forest
- **significantly modifies late-time structure formation:**
 - group/cluster bimodality of core entropy values
 - may suppress Sunyaev-Zel'dovich power spectrum
 - dwarf formation: “missing satellite” problem, void phenomenon
- **explains puzzles in high-energy astrophysics:**
 - TeV blazars can evolve like quasars
 - extragalactic gamma-ray background at $E \gtrsim 10$ GeV
 - invalidates intergalactic B -constraints from blazar spectra

